ELSEVIER

Journal of Chromatography B, 703 (1997) 139–145

JOURNAL OF CHROMATOGRAPHY B

Discrimination limit for purity test of human insulin by capillary electrophoresis

Chikako Yomota[a], Yasunobu Matsumoto[a], Satoshi Okada[a], Yuzuru Hayashi[b,*], Rieko Matsuda[b]

[a]*Osaka Branch, National Institute of Health Sciences, Hoenzaka1-1-43, Chuo-ku, Osaka 540, Japan*
[b]*National Institute of Health Sciences, 1-18-1 Kami-Yoga, Setagaya, Tokyo 158, Japan*

Received 9 June 1997; received in revised form 12 August 1997; accepted 12 August 1997

Abstract

Because of the inevitable noise in instrumental analysis, a purity test can overlook an illegitimate drug that contains an undesired substance in a higher amount than the prescribed limit. The lowest (average) amount of undesired substance which leads to the right results of the purity test with 95% probability is referred to here as 95% discrimination limit. This paper presents a method for predicting the discrimination limit for the purity test of human insulin in capillary electrophoresis (CE). The theory and experiments show that if the legitimate limit of a degradation product (desamido insulin) is 3.0% of the total amount of the insulin formulation, the 95% discrimination limit in the CE system used in this study is 3.24% desamido insulin. Since the statistical aspects of the purity test are provided by the interpretation of the baseline fluctuation in the instrument, the usual strategy to repeat the instrumental analysis on the same samples is unnecessary in the present study.

Keywords: Discrimination limit; Insulin

1. Introduction

Human insulin is liable to deamidation at position A-21. US Pharmacopeia (USP) stipulates the purity test for human insulin by liquid chromatography as follows: the relative amount of desamido insulin (A-21DHI) must not be more than 3% of the total amount of insulin and desamindo insulin [1]. The insulin degradation product has been analyzed by liquid chromatography [2–5] and capillary electrophoresis (CE) [5–7].

The purity test should signal rejection for the illegitimate drug that contains A-21DHI in amounts larger than the USP limit (i.e. 3%). Nevertheless, instrumental responses are inevitably disturbed by noise, which blurs the results of the test. The gray line of Fig. 1 shows the normal distribution of the test results, Y, with the relative mean amount of undesired substance, $\bar{Y}$. $\bar{Y}$ is slightly higher than the USP limit (3%) so that the test can find the irregularity with 95% probability. This amount is referred to here as 95% discrimination limit. The solid line of Fig. 1 shows the dependence of the probability for the right answers on the mean amount, $\bar{Y}$, of undesired substance. If the amount is equal to the USP limit, the opposite conclusions ($Y>3\%$ or $Y<3\%$)

*Corresponding author.

0378-4347/97/$17.00
PII S0378-4347(97)00417-9

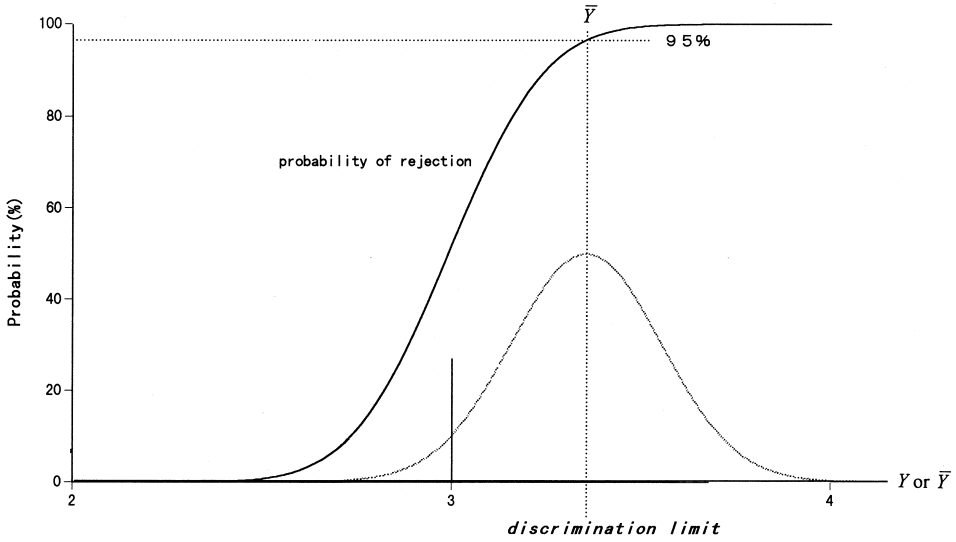

Fig. 1. Distribution of the results from the purity test at 95% discrimination limit (gray line) and dependence of the probability for the purity test to find the irregularity as a function of the relative mean amount of undesired substance, $\bar{Y}$ (solid line). The distribution of the test results is assumed to be constant (homoscedastic).

will be drawn with equal probability (50%). However, if the amount is much greater than the limit, the test can find the irregularity with almost 100%.

The aim of this paper is to determine the discrimination limit of the purity test for the desamido insulin in a CE apparatus. The discrimination limit depends to a large extent on the statistical reliability (repeatability) of the analytical instrument used for the test. In general, the more precise the test, the smaller the discrimination limit, as long as the same probability for the right judgment is referred to (here, 95%). The discrimination limit is a general concept covering the limit of detection, [8] but there have been few publications about its applications in analytical chemistry [8–10]. The practical example of the discrimination limit in HPLC was first demonstrated in our previous study [10] where two HPLC responses were compared. The present study is concerned with the relative amount of desamido insulin and the regulation limit (3%).

If the S.D. (standard deviation) of the results of the test is exactly estimated, the 95% discrimination limit can easily be calculated on the assumption of the normal distribution of the test results as shown in Fig. 1. Usually, an S.D. estimate can be obtained from repeated experiments. However, this straightforward method poses a critical problem. If the S.D. estimate is obtained from 50 experiments ($n=50$), 95% of all the possible S.D. estimates to be obtained in this way scatter over the range from 80 to 120% of the true value. The error of $\pm 20\%$ will be acceptable in many cases in analytical chemistry, but the number of repetitions ($n=50$) is not realistic for slow analyses. For a practical number of replicates (e.g., $n=5$), the scattering is unsuitable (31–150%). This fact can well be explained in statistics in terms of the chi-square distribution.

Instead, this paper employs a probability theory for predicting the uncertainty of measurement, i.e., S.D. or relative standard deviation (R.S.D.) value of instrumental responses [11–13]. The corresponding scattering of the S.D. values predicted is 78–122% from a single baseline of 2048 data points [12,13]. If the data acquisition rate is 5 Hz in a CE system, it takes no more than 7 min to collect the 2048 data. The statistical reliability of this prediction can be enhanced further by analyzing more baselines [12,13].

2. Experimental

2.1. Materials and sample preparation

The human insulin reference standard of National Institute of Health Sciences, Japan, was used as human insulin. A-21DHI was prepared by storing the human insulin in 0.01 *M* HCl at 40°C for 48 h [14]. The illegal model samples were prepared by mixing the human insulin solution and A-21DHI solution in an appropriate ratio.

2.2. CE analysis

The CE instrument used was a Photal CAPI-3000 CE apparatus (Otsuka Electronics) equipped with a fused-silica capillary of 50 μm I.D. and 50 cm total length (37.5 cm effective length) and photo-diode array detector. The capillary temperature was maintained at 25°C and the wavelength of the detector was 214 nm. The sampling interval of the analog-to-digital converter used was 345 ms. The samples were introduced by hydrostatic injections from a height of 10 mm over 10 s. The mobile phase consisted of 0.1 *M* tricine buffer, 0.02 *M* NaCl, 1 *M* urea and 0.45 *M* ethyleneglycol at pH 8.1. The applied voltage for separation was 7 kV (140 V/cm).

In the concentration ranges of urea and ethyleneglycol in our study, the addition of urea to the mobile phase sharpened the CE peaks, but increased the noise level. Ethyleneglycol sharpened the peak shape by increasing the mobile phase viscosity and in turn suppressing the diffusion of the solute.

2.3. Purity test of desamido insulin content

The result, *Y*, of the purity test is expressed as the ratio of the CE response for the desamido insulin, A_2 (entire peak area), to the total responses for insulin, A_1, and desamido insulin, A_2: $Y = A_2/(A_1 + A_2)$. The entire peak areas, A_1 and A_2, are obtained by drawing the zero line of the integration, if necessary, obliquely along the baseline drift.

For the prediction of the S.D. of the test results, the CE baselines and signals of the target materials are processed as follows. The long-term drift present in the baseline is eliminated by the least squares fitting of a linear function. The model fitting to the corrected baselines produces the noise parameters necessary for the uncertainty prediction (see below). According to the peak shape, the signal integration domain is set as 95 data points for insulin and 29 data points for A-21DHI around the respective signal maximums. The zero level from which the relative intensities are summed in the integration is the average of ten baseline intensities before the zero point. The integration starts at the data point next to the zero point.

In theory, the discrimination limit can be calculated from one electropherogram (or a signal shape). For better prediction, the average of six power spectra and the signal shape that is closest to the average of six CE traces are used. The model samples for the illegal drugs (see Fig. 4) were prepared according to the discrimination limit based on the above signal shape.

3. Theory

3.1. Prediction of discrimination limit

It is assumed here that the results, *Y*, of the purity test have a normal distribution. If the difference between the mean of the results, $\overline{Y}$, and regulation limit, Y_L, is 1.6 times as large as the standard deviation, *s*, of the results, *Y*, the probability of the right result is 95% (see Fig. 1):

$$\overline{Y} - Y_L = ks \tag{1}$$

where $k = 1.6$ and $Y_L = 0.03$.

Given the S.D., *s*, of the test results, we can find the 95% discrimination limit, $\overline{Y}$ from Eq. (1). The first purpose of this subsection is to express the S.D., *s*, of the test results, $A_2/(A_1 + A_2)$, as a function of the variances of the individual responses, A_1 and A_2, for insulin and its degradation product, respectively. Finally, the discrimination limit is derived from the S.D. values of the test results. The theoretical background to predict the variances for A_1 and A_2 is briefly reviewed below.

The R.S.D. of quotients, $A_2/(A_1 + A_2)$, is known in statistics, if the numerator and denominator in the

quotients are probabilistically independent [15]. In our situation, however, they have the response, A_2, in common and are more or less correlated. The R.S.D. values with such correlation has already been given as: [16]

$$\frac{s}{\overline{A_2}/(\overline{A_1}+\overline{A_2})} = \left\{ \frac{\mathrm{Var}(A_1)}{\overline{A_1}^2} + \frac{\mathrm{Var}(A_2)}{\overline{A_2}^2} \right\}^{1/2} \frac{\overline{A_1}}{\overline{A_1}+\overline{A_2}} \tag{2}$$

where Var() is the variance of the random variable in the parentheses and $\overline{A_i}$ is the mean of the responses, A_i (i=1 or 2). Therefore, the S.D. of the test results can be described as:

$$s = \left\{ \frac{\mathrm{Var}(A_1)}{\overline{A_1}^2} + \frac{\mathrm{Var}(A_2)}{\overline{A_2}^2} \right\}^{1/2} \frac{\overline{A_1 A_2}}{(\overline{A_1}+\overline{A_2})^2} \tag{3}$$

The simple description of the mean results is assumed: $\overline{Y} = \overline{A_2}/(\overline{A_1}+\overline{A_2})$. Noticing that $\overline{A_1}/(\overline{A_1}+\overline{A_2}) = 1-\overline{Y}$, we can obtain:

$$s = \{\mathrm{Var}(A_1)\overline{Y^2} + \mathrm{Var}(A_2)(1-\overline{Y})^2\}^{1/2} \frac{1}{\overline{A_1}+\overline{A_2}} \tag{4}$$

Then, Eq. (1) takes the form:

$$\overline{Y} - Y_L = k\left\{\mathrm{Var}(A_1)\overline{Y^2} + \mathrm{Var}(A_2)(1-\overline{Y})^2\right\}^{1/2} \frac{1}{\overline{A_1}+\overline{A_2}} \tag{5}$$

Solving the above equation for $\overline{Y}$, we can obtain the quadratic equation:

$$a\overline{Y^2} + 2b\overline{Y} + c = 0 \tag{6}$$

where

$$a = (\overline{A_1}+\overline{A_2})^2 - k^2\mathrm{Var}(A_1) - k^2\mathrm{Var}(A_2) \tag{7a}$$

$$b - (\overline{A_1}+\overline{A_2})^2 Y_L + k^2\mathrm{Var}(A_2) \tag{7b}$$

$$c = (\overline{A_1}+\overline{A_2})^2 Y_L^2 - k^2\mathrm{Var}(A_2) \tag{7c}$$

The answer is:

$$\overline{Y} = \frac{-b+\sqrt{b^2-ac}}{a} \tag{8}$$

Naturally, the discrimination limit, $\overline{Y}$, should increase with increasing k. The computer simulation shows that the positive sign of the square root of Eq. (8) is correct.

To calculate Eq. (8), we need to know $\mathrm{Var}(A_1)$, $\mathrm{Var}(A_2)$, $\overline{A_1}$ and $\overline{A_2}$. The means of the responses, $\overline{A_1}$ and $\overline{A_2}$, can be obtained from the CE measurements and the variances, $\mathrm{Var}(A_1)$ and $\mathrm{Var}(A_2)$, as described below. The regulation limit, Y_L, is defined by regulatory authorities and the k value is determined according to the strictness of the purity test.

3.2. Response uncertainty in CE

The contents of this subsection were described elsewhere in detail [11–13]. The 'false area' created by the baseline alone without samples can be regarded as the major cause of the response uncertainty at low sample concentrations. At high sample concentrations, however, the injection error, I, is predominant over the false area. The variance, σ_M^2, of responses can be described as:

$$\begin{aligned}\sigma_M^2 = {} & (k_f - k_c)\tilde{w}^2 \text{ (first term)} \\ & + \frac{1}{(1-\rho)^2}\left(k_f - k_c - 2\rho\frac{1-\rho^{k_f-k_c}}{1-\rho} \right. \\ & \left. + \rho^2\frac{1-\rho^{2(k_f-k_c)}}{1-\rho^2} \right)\tilde{m}^2 \text{ (second term)} \\ & + I^2 E[\overline{A_i}]^2 \text{ (third term)}\end{aligned} \tag{9}$$

where $\tilde{w}$ means the S.D. of the white noise and $\tilde{m}$ and ρ are the S.D. and auto-correlation parameter of the Markov process, respectively. The signal integration starts at k_c+1 and ends at k_f (the data points in the integration domain are k_f-k_c; here, $k_c=0$). The first term of Eq. (9) corresponds to the error from the white noise in the integration domain, the second term is the error from the Markov process in the integration domain and the third term is the injection error.

Noise parameters, $\tilde{w}$, $\tilde{m}$ and ρ, are all determined by the least-squares fitting of the theoretical power spectrum of the model process to the actual power spectrum of a baseline [11–13]. The injection error, I, can be considered to be canceled out in the quotient, $A_2/(A_1+A_2)$, and is omitted for the prediction of the discrimination limit ($I=0$). Although the oblique zero line is used for the integration in

experiments, the horizontal zero line is assumed in Eq. (9) for the theoretical prediction. This is because the long-term drift in the baselines is eliminated in the preprocess (see above).

The signal intensity is integrated or summed relatively to the zero level. In practice, the zero level itself is subject to baseline fluctuation. The error of the zero level setting can be described as: [17]

$$\sigma_Z^2 = \frac{(k_f - k_c)^2}{b}\tilde{w}^2 + \frac{(k_f - k_c)^2}{b^2(1-\rho)^2}\left(b - 2\rho\frac{1-\rho^b}{1-\rho} + \rho^2\frac{1-\rho^{2b}}{1-\rho^2}\right)\tilde{m}^2 \quad (10)$$

where b denotes the number of consecutive data points $(-b+1, 0)$ over which the baseline noise is averaged for the zero level.

The squared S.D., σ^2, of the integrated responses with the zero level setting takes the form:

$$\sigma^2 = \sigma_M^2 + \sigma_Z^2 \quad (11)$$

This equation is used throughout this paper.

4. Results and discussion

Fig. 2 shows an example of the electropherograms of the human insulin degraded at the acidic condition described in Section 2.1. Peaks 1 and 2 correspond to the insulin and A-21DHI, respectively. They are baseline-separated and the entire peak areas, A_1 and A_2, can be measured independently of each other. The result of the purity test is $A_2/(A_1 + A_2)$.

The power spectral density of the baselines in the CE apparatus is shown in Fig. 3. It is the average of the power densities from six baselines of 2048 data points each. The simplex least squares provides the noise parameters by fitting the model power density to the observed power density shown in Fig. 3: $\tilde{w} = 5.47 \cdot 10^{-5}$; $\tilde{m} = 5.27 \cdot 10^{-6}$; $\rho = 0.9992$.

The power of the waves present in the baselines decreases with increasing frequency up to 0.03 Hz and looks like a flicker noise or $1/f$ noise (f means frequency) (see Fig. 3). This indicates that the baseline in the CE apparatus has auto-correlation.

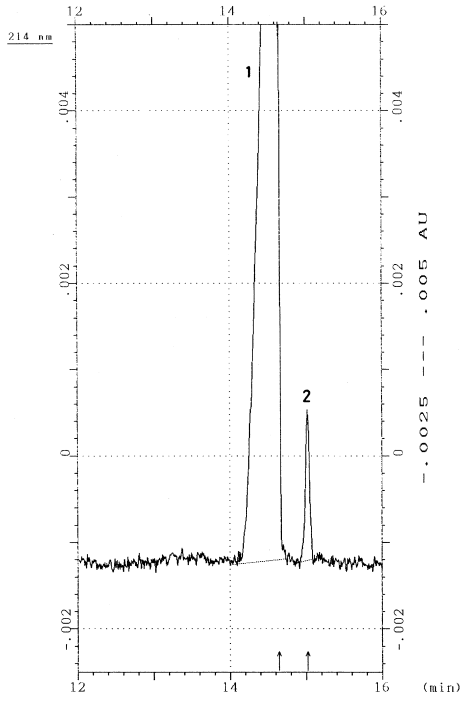

Fig. 2. Electropherogram of human insulin. The experimental conditions are given in the text. The arrows denote the signal maxima for the insulin (peak 1) and A-21DHI (peak 2; 2.30%), respectively.

That is, the noise intensities are not mutually independent along the time axis. In addition, the $1/f$ fluctuation has been observed in a surprising number

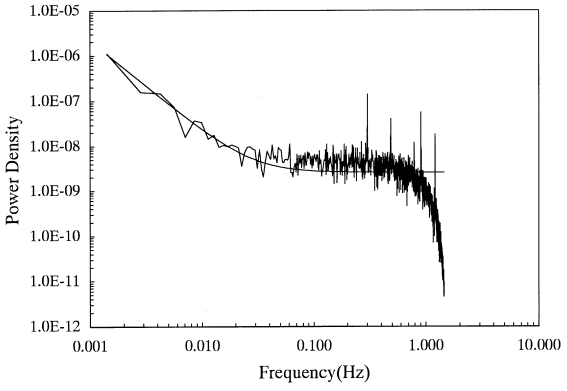

Fig. 3. Power spectral density of the CE baselines. The noisy line denotes the observed power density and the smooth one is the best fit of the baseline model (for the model, see the text). The experimental conditions are the same as in Fig. 2.

of natural phenomena [18] as well as in analytical instruments [13,19,20].

The horizontal line around 0.5 Hz shows the white noise ($\tilde{w}^2 = 3 \cdot 10^{-9}$). The observed power spectral density decreases abruptly over 1 Hz possibly because of a low pass filter originally installed in the CE apparatus. This steep decrease is negligible in the uncertainty prediction, since the high frequency noises (>1 Hz) are canceled out by each other in the signal integration (33 s for insulin and 10 s for desamido insulin).

The instrumental noise is often approximated by the white noise in analytical chemistry [21]. The S.D. of integrated white noise can easily be calculated from the S.D. of the original white noise [22]. In general, it is not so easy to predict the response S.D. from the auto-correlated baselines as from the white noise. Fortunately, the baseline fluctuation resembles the mixture of the well-defined random processes called the white noise (time-independent process) and Markov process (time-correlated one) and the S.D. of the integrated baseline intensities can be predicted from the noise and signal parameters, $\tilde{w}$, $\tilde{m}$, ρ, A_i, k_c and k_f [11–13]. This is why the repetition of measurement can be dispensed with in our study.

From the prediction theory, it follows that in the CE system used in this study, the 95% discrimination limit for the purity test of human insulin is 3.24% A-21DHI and that the 99.87% discrimination limit is 3.44%. The theory is in good agreement with the experiment as shown in Fig. 4. The A-21DHI contents (3.28 and 3.47%) of the illegal model samples used in Fig. 4 are close to the above discrimination limits, respectively. For the 95% discrimination limit, the risk of overlooking the irregularity of the formulation is 5% and Fig. 4A shows that two results out of twenty fall below the regulation limit of 3%. For the sample containing an even more A-21DHI than the 95% discrimination limit (actually, 99.87% discrimination limit; see Fig. 4B), the number of misjudgments is 0.026 in theory ($=20 \times 0.0013$) and no misjudgments are observed in the experiments.

Even if the 95% discrimination limit given above is true, the experimental results scatter due to the finite number of trials in Fig. 4A ($n=20$). According to the combinatorial theory, the probability for no results below the limit is 0.358, that for one result

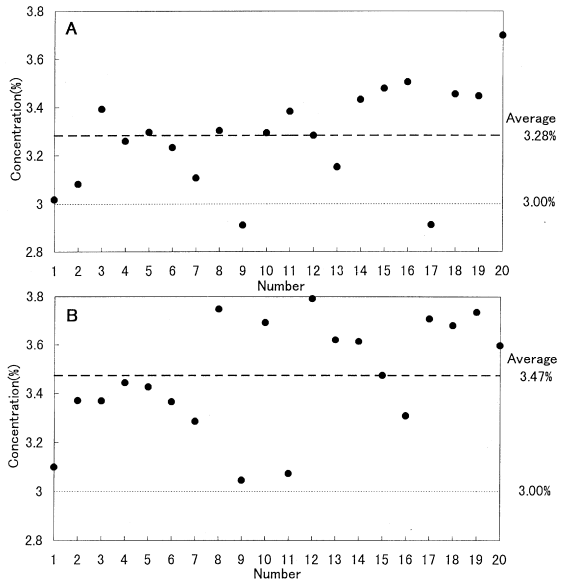

Fig. 4. Results of the purity test at the A-21DHI contents of 3.28% (A) and 3.47% (B). Twenty tests (number 1–20) are performed. The experimental conditions are the same as in Fig. 2.

(theoretical) is 0.377, that for two 0.189 and for three 0.06. The experimental proof for or against the theory of the discrimination limit would be difficult except for a large number of replicates. However, the prediction theory can be considered quite satisfactory on the grounds of the results of Fig. 4 and other evidence described previously [11–13].

The theoretical S.D. values of the test results of Fig. 4A and B are both 0.00149 and the observed values are 0.00205 for the former and 0.00227 for the latter. If the theoretical S.D. were imprecise, the prediction of the discrimination limit based on these theoretical values would have been disastrous. The measurement R.S.D. value increases with decreasing sample concentration. The discrimination limit depends on the concentration of the target materials. If the sample concentration is lower than that of Fig. 4, the 95 and 99.87% discrimination limits would be larger than in this study.

The discrimination limit entirely depends on the statistical reliability of an analytical instrument used in a laboratory, generally varying from instrument to instrument. Therefore, an analyst has to know the precision of his or her instrument.

The discrimination limit taken in this paper corre-

sponds to the consumer's risk in statistical terminology, and the producer's risk can also be treated in a similar way.

Acknowledgements

This work was supported by Japan Health Sciences Foundation.

References

[1] United States Pharmacopeia 23, US Pharmacopeial Convention, MD, 1995.
[2] H.W. Smith, L.M. Atkins, D.A. Brinkley, W.G. Richardson, D.J. Miner, J. Chromatogr. 8 (1985) 419.
[3] D.M. Smith, R.M. Venable, J. Collins, J. Chromatogr. Sci. 23 (1985) 81.
[4] B.V. Fisher, D. Smith, J. Pharm. Biomed. Anal. 3 (1986) 377.
[5] C. Yomota, Y. Yoshii, T. Takahata, S. Okada, J. Chromatogr. A 721 (1996) 89.
[6] S. Nitta, H. Sasagawa, C. Yomota, S. Okada, Chromatographia 13 (1992) 339.
[7] R.G. Nielsen, G.S. Sittampalam, E.C. Pickard, Anal. Biochem. 177 (1989) 20.
[8] L.A. Currie, in: L.A. Currie (Ed.), Detection in Analytical Chemistry. Importance, Theory, and Practice, American Chemical Society, Washington, DC, 1988,
[9] R. Ferrús, M.R. Egea, Anal. Chim. Acta 287 (1994) 119.
[10] Y. Hayashi, R. Matsuda, J. Pharm. Biomed. Anal. 15 (1997) 697.
[11] Y. Hayashi, R. Matsuda, Anal. Chem. 66 (1994) 2874.
[12] Y. Hayashi, R. Matsuda, R.B. Poe, Analyst 121 (1996) 591.
[13] Y. Hayashi, R. Matsuda, R.B. Poe, J. Chromatogr. A 722 (1996) 157.
[14] J. Brange, Galenics of Insulin, Springer, Berlin, 1987.
[15] R.A. Day, A.L. Underwood, Quantitative Analysis, Pentice Hall, Engelwood Cliffs, NJ, 1991.
[16] Y. Hayashi, R. Matsuda, Anal. Sci. 10 (1994) 881.
[17] R.B. Poe, Y. Hayashi, R. Matsuda, Anal. Sci., in press.
[18] T. Musha, The world of fluctuation (Yuragi no sekai), Kodansha, Tokyo, 1993.
[19] A. Bezegh, J. Janata, Anal. Chem. 59 (1987) 494A.
[20] H.C. Smit, H.L. Walg, Chromatographia 8 (1975) 311.
[21] G. Bergmann, B. von Oepen, P. Zinn, Anal. Chem. 59 (1987) 2522.
[22] Y. Hayashi, R. Matsuda, in: P.R. Brown, E. Grushka (Eds.), Advances in Chromatography, Marcel Dekker, New York, 1994, p. 347.